Original Article

Biosynthesis of Iron Oxide Nanoparticles Using Ethyl Acetate Extract of *Chaetomium cupreum* and their Anticancer Activity

Nazir Ahmad Wani, Waseem Iqbal Khanday[1], Sharmila Tirumale

Department of Microbiology and Biotechnology, Jnanabharathi Campus, Bangalore University, Bengaluru, Karnataka, [1]Research Centre in Biotechnology, MGR College, Hosur, Tamil Nadu, India

Abstract

Background: The biosynthesis of iron oxide nanoparticle (NP) formation was carried out using ethyl acetate extract of fungus *Chaetomium cupreum* as reducing agents. The *C. cupreum* contains azaphilones pigments which poses various biological activities. **Objectives:** The synthesis of iron oxide NP and their anticancer potential was investigated. **Materials and Methods:** The anticancer activities of biosynthesized iron oxide NP were evaluated using tetrazolium bromide assay, measurement of reactive oxygen species (ROS), mitochondrial membrane potential (MMP), and inhibition of tumorsphere formation. **Results:** In the present study, the X-ray diffraction shows the presence of gamma phase iron oxide NP withe the type of Fe_2O_3. The anticancer potential of iron oxide NP was investigated against human breast cancer cell line. The anticancer activity of biosynthesized iron oxide NP against MCF-7 was 20.5, 30.5, 41.1, 55.3 67.5, and 75.25 at 50 µg/ml after 1, 5, 10, 15, 20, and 24 h of treatment, respectively. The results showed that Fe_2O_3 NP induced ROS generation to 68.22% at the concentration of 25 µg/ml and 83.66% at 50 µg/ml as compared to 48.22 in control after 15 h of treatment. The results showed that Fe_2O_3 NP treatment increased depolarization MMP to 8.52% at 25 µg/ml and 10.74% at 50 µg/ml as compared to 6.35% in untreated cells after 24 h. Thus, treatment with Fe_2O_3 NPs showed significant inhibition of MCF-7 tumorsphere formation at higher concentration. **Conclusion:** The biosynthesized iron oxide NP using ethyl acetate extract of *C. cupreum* exhibit significant anticancer activity.

Keywords: *Chaetomium cupreum,* diffraction, iron oxide nanoparticle, myconanotechnology, spectroscopy

Introduction

Nanotechnology is one of the rapidly growing research fields with its applications in science to produce materials in nanoscale level (1–100 nm). Nanotechnology is presently used in the field of biology, pharmacology, medicine, electronics, and tissue engineering.[1] In recent years, the development of green nanotechnology approach has attracted the researchers which involves the nontoxic method for the synthesis of nanoparticles (NPs). In green nanotechnology method, the metal oxide NPs are biosynthesized using plants, fungi, algae with various shapes.[2,3] In this green approach, the biomolecules present in natural extract acts as reducing and capping agents.[4] Green synthesis of NPs is an eco-friendly, economic, simple method, and eliminates the use of harmful reagents which is more advantageous than the conventional physical and chemical methods.[5,6] The exploration of fungi in nano-biotechnology research is very important. The fungi have attracted more attention for the biological production of metal NPs because of their toleration and metal bioaccumulation potential.[7]

Fungi are microorganisms containing different kinds of secondary metabolites with their applications in pharmaceutical and medicinal industry. The *Chaetomium* are the largest genous of saprophytic ascomycetes with chaetomiaceae family. The *Chaetomium* was first reported in 1817 by Kunze and more than 350 chaetomium species are known.[8] This species is widely distributed in soil, marine, hair, textile, plant seeds, and other substances rich in cellulose. The *Chaetomium cupreum* is distinguished from other *Chaetomium* species due to the

Access this article online

Quick Response Code:

Website: www.matrixscipharma.org

DOI: 10.4103/MTSP.MTSP_6_20

Address for correspondence: Dr. Nazir Ahmad Wani, Department of Microbiology and Biotechnology, Jnanabharathi Campus, Bangalore University, Bengaluru - 560 056, Karnataka, India.
E-mail: nazirwani100@gmail.com

How to cite this article: Wani NA, Khanday WI, Tirumale S. Biosynthesis of iron oxide nanoparticles using ethyl acetate extract of *Chaetomium cupreum* and their anticancer activity. Matrix Sci Pharma 2020;4:23-30.

Received: 27-May-2020 **Accepted:** 03-Jun-2020 **Available Online:** 30-Nov-2020

presence of boat-shaped ascospores and copper color thin long hairs on the outer surface of the perithecia.[9] As there are no reports of green synthesis of NPs from *C. cupreum* extracts. Therefore, an attempt was made in this study to green synthesize the iron oxide NPs from the ethyl acetate extract of *C. cupreum*.

Materials and Methods

Chemicals

The chemicals used are ferrous sulfate ($FeSO_4$), sodium hydroxide (NaOH), potato dextrose agar, nutrient agar, dimethyl sulfoxide, tetrazolium bromide dye, ethyl acetate, JC-1 dye, Deficiência Combinada de Hormônios Hipofisários-DA dye.

Preparation of ethyl acetate extract

The culture of *C. cupreum* was procured from the National Fungal Culture Collection of India (NFCCI), Agharkar Research Institute, Pune, India, with accession No. NFCCI-3117. The extraction of secondary metabolites from fungus broth using liquid-liquid method as described in our previous articles.[10]

Biosynthesis of iron oxide nanoparticle

The biosynthesis of Fe_2O_3 NP was described by Shahwan *et al*.[11] The fungal extract solution was prepared by dissolving 5.0 g of ethyl acetate powder in 250 ml of dist. water and heated for 60 min at 70°C. A solution containing dissolved ethyl acetate extract of *C. cupreum* was obtained by filtration. The iron solution was prepared by heating 2 g of $FeSO_4$ powder in 100 ml of distilled water at 50°C for 12 min. Then, NaOH solution was prepared by dissolving 1.20 g NaOH in 100 ml and heated at 50°C for 15 min. In 100 ml of $FeSO_4$ solution, 50 ml of NaOH was added to balance the pH of the solution. Then, from $FeSO_4$ NaOH solution, 100 ml was added to 50 ml of ethyl acetate extract solution and the solution was heated at 30°C for 60 min. Then, the solution was heated in a microwave at 150°C for 2 min. After overnight incubation in an oven black solution of iron oxide, NPs were obtained. The morphology and structural analysis were evaluated through field emission scanning electron microscopy (FESEM), energy dispersed X-ray spectroscopy (EDX), and X-ray diffraction (XRD).

Anticancer activity

The human breast cancer cell line (MCF-7) was procured from the National Cell Culture Science, Pune, India. The MCF-7 cells were maintained in Dulbecco's Modified Eagle Medium (DMEM) and incubated in Co_2 incubator at 37°C. The anticancer activity of Fe_2O_3 NPs on MCF-7 cells by MTT dye 3-(4,5-dimethylthiazol-2-yl)-2,5 dihenyl tetrazolium bromide.[12] A volume of 200 µl of cell suspension (1×10^4 cells/well) were poured in microtiter plate and plate was incubated at 37C for 24 h hours in a 5% Co_2 incubator until 95% confluence. After 24 h, 200 µl of fresh media containing Fe_2O_3 NPs were added and incubated overnight. After incubation, 20 µl MTT dye was added and covered with aluminum foil and kept in dark for 3 h. Then, formosan crystals formed were lysed by adding 200 µl of dimethyl sulfoxide and absorbance was recorded at 585 nm using micro plate reader. The percentage of cell viability was calculated as (OD of treated cells/OD of control cells) × 100.

Morphological observation of MCF-7 cells

For morphology detection MCF-7 cells were seeded and incubated incubated with or without Fe_2O_3 NPs for overnight. The phase contrast microscope at ×200 was used for morphology observation.

4,6-Diamidino-2-phenylindole) staining

For 4,6-diamidino-2-phenylindole (DAPI) staining, MCF-7 was treated with or without Fe_2O_3 NPs for 24 h at 37°C. The treated cells were washed with Phosphate buffer saline (PBS) and stained with DAPI and incubated at 37C for 15 min and observed under fluorescent microscope.

Acridine orange and ethidium bromide stain

The MCF-7 cells were treated with or without Fe_2O_3 NPs and incubated at 37°C for night. Then, 0.5 ml of acridine orange/ethidium bromide (AO/EtBr) was added and left for 5 min and absorbed under fluorescent microscope at × 200 magnification.

Measurement of reactive oxygen species

The reactive oxygen species (ROS) level of living cells was measured using 2,7-dichlorodihydrofluorescein diacetate (DCFH-DA).[13] A volume of 200 µl cell suspension (1×10^4 cells/ml) were seeded in 96 microtiter plate and incubated for 24 h at 37°C. Then, cells were treated with or without Fe_2O_3 NP and incubated for 15 h. Then, 100 µl of DCFH-DA (µM) were added and further incubated for 30 min. The fluorescence at excitation (485) and emission wavelength (535) was recorded using microplate reader.

Measurement of mitochondrial membrane potential

The mitochondrial membrane potential (MMP) in MCF-7 cells using JC-1 (5,5,6,6-tetrachloro-1,1,3,3-tetraethylbenzimidazolyl arbocyanine iodide) method.[14] The 200 µl (1×10^4 cells/ml) of MCF-7 cells were plated in DMEM media on microtiter plate. Then, cells were treated with Fe_2O_3 NP and further incubated for another 24 h at 37°C. Then, cells were washed with PBS and 100 µl of JC-1 dye was added and again incubated for 20 min. The monomer fluorescence was measured with excitation 525 nm and emission wavelength of 590 nm using fluorescent spectrophotometer.

Tumor sphere formation assay

The tumorsphere formation examined by Lu method.[15] The MCF-7 cells were cultured in six well plate in serum-free DMEM (F12) in a cell suspension of 1000 cells/ml. The DMEM/F12 media contains human recombinant epidermal growth factor (20 ng/ml), basic fibroblast growth factor (20 ng/ml), heparin (4 µg/ml), insulin (5 µg/ml), and 1% penicillin-streptomycin. The tumorsphere formation was detected by treating MCF-7 cells with Fe_2O_3 NPs and control was maintained without NPs. The wells were monitored and images of tumorsphere formation were captured every day till 7 days of incubation.

Statistical analysis

The two-way analysis of variance followed by Tukey's multiple comparison test with graph pad prism 6 software were used. The results were expressed as mean ± standard deviation of three replicates. The $P < 0.05$ was considered as statistically significant.

Results

Extraction and biosynthesis of iron oxide nanoparticle

The extraction of secondary metabolites is shown in Figure 1. The biosynthesis of Fe_2O_3 NP involves ethyl acetate extract of *C. cupreum* [Figure 2].

Characterization of iron oxide nanoparticle

The XRD pattern shows the presence of gamma phase, maghemite (γ-Fe_2O_3) JCPDS 39–1346 [Figure 3]. Thus, the XRD report proves the presence of iron oxide NPs with the type of Fe_2O_3. The iron oxide NPs were obtained in black color. The NPs were spherical in shape and their average size measured was 25 nm. The particle size was calculated from Debye-Scherrer formula in the X-ray method. The elemental composition was obtained by EDX spectroscopy spectrum which includes iron, oxygen, silicon, and carbon [Figure 4a and b]. The carbon and silicon were the contaminating elements with very low concentration in the sample. The iron oxide NPs images were obtained as big clusters at various magnifications shown by FESEM [Figure 5].

Anticancer activity

The anticancer activity of Fe_2O_3 NPs on MCF-7 cell line is presented in Figure 6. The highest anticancer activity of Fe_2O_3

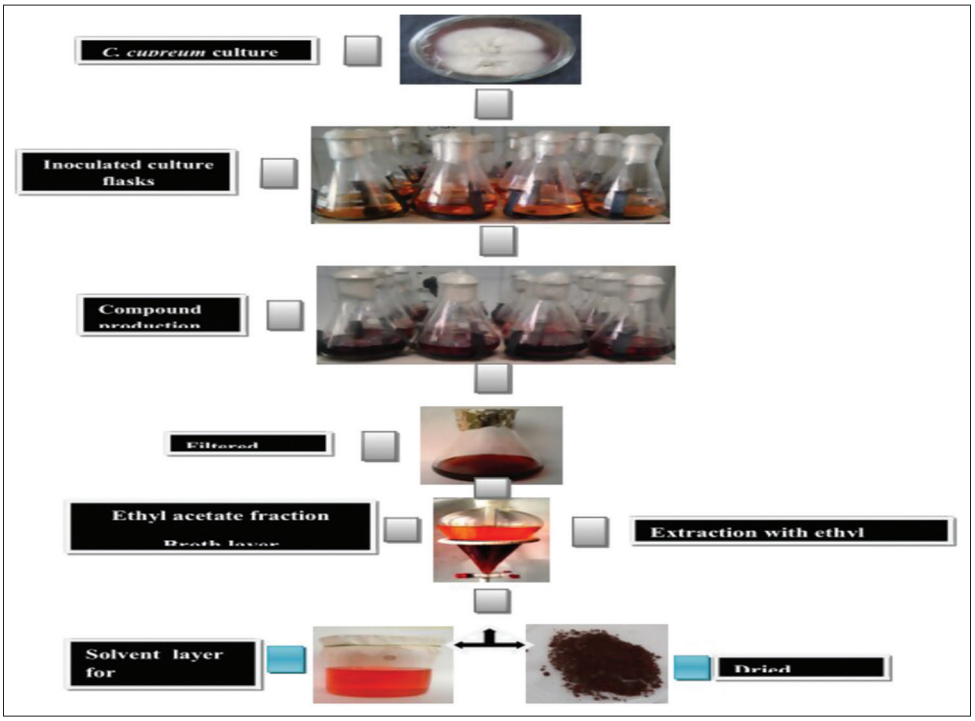

Figure 1: Extraction of compounds from *Chaetomium cupreum*

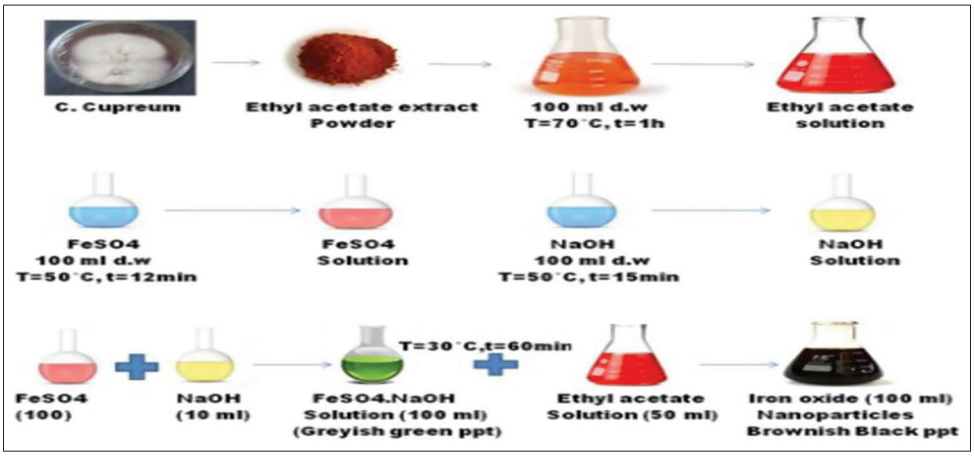

Figure 2: Biosynthesis of iron oxide nanoparticles

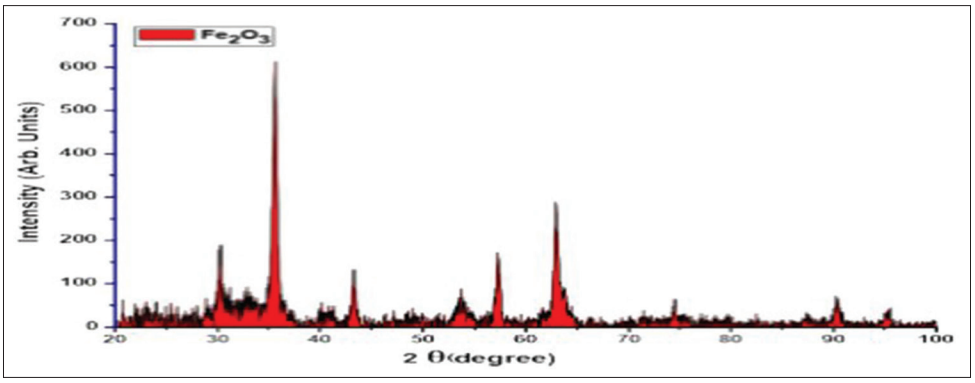

Figure 3: X-ray diffraction spectrum of Fe2O$_3$ nanoparticle

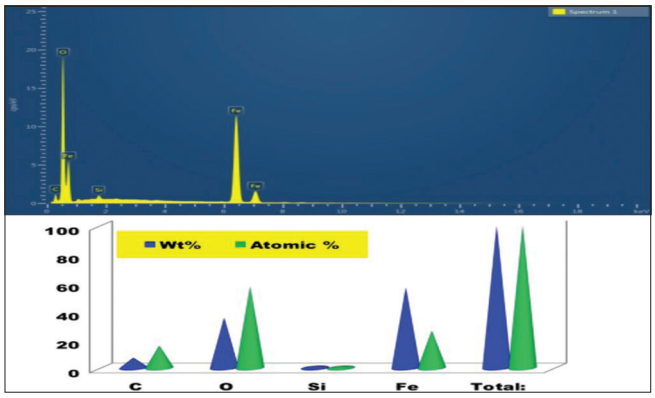

Figure 4a: Energy dispersed X ray spectrum of Fe2O3 nanoparticle. **Figure 4b:** Elemental composition of Fe2O3 NP

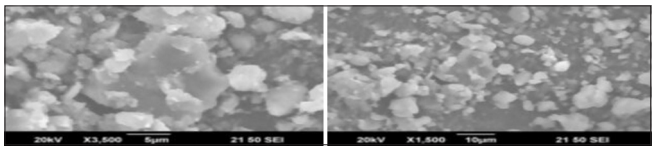

Figure 5: Field emission scanning electron microscopy images of iron oxide nanoparticles

NP against MCF-7 cell line was 20.5, 30.5, 41.1, 55.3 67.5, and 75.25 at the concentration of 50 µg/ml after 1, 5, 10, 15, 20, and 24 h of treatment, respectively. Similarly, the anticancer activity of Fe_2O_3 against MCF-7 cell line was 14.25, 26.75, 34.5, 42, 49.5, and 55.56 after 1, 5, 10, 15, 20, 24 h at the concentration of 25 µg/ml. Whereas at lower concentrations at 12.5, 6.25, 3.13, and 1.56, there was gradual decrease in cytotoxic activity. The Fe_2O_3 NP shows the IC_{50}-20 µg/ml concentration against MCF-7 cells.

Morphological observation

The cell death can be observed using fluorescent staining technique. In DAPI staining, the live cells appear blue whereas dead cells show white fluorescence [Figure 7]. Similarly, in case of AO/EtBr staining, the live cells have normal morphology and took up AO produce green fluorescence whereas dead cells have altered morphology and took up EtBr stain and produce orange fluorescence [Figure 7]. It was found that control MCF-7 cells shows normal morphology and normal proliferation growth. In case of Fe_2O_3 NP treatment, the dead and dying cells get detached from the surface of well plate and float in media. These dead cells have lost their morphology and appeared smaller and round in shape. Thus, these results indicated that Fe_2O_3 NP treatment exhibited cytotoxicity against breast cancer cells.

Measurement of reactive oxygen species

The Fe_2O_3 NP treatment induced ROS production in MCF-7 cells. The results showed that Fe_2O_3 NP induced ROS generation to 68.22% at 25 µg/ml and 83.66% at 50 µg/ml as compared to 48.22 in control after 15 h of treatment [Figure 8a and b]. The ROS production was significantly ($P < 0.05$) increased at higher concentration in comparison to control cells. Further, the results indicate that Fe_2O_3 NPs are able to induce ROS generation in breast cancer cells.

Measurement of mitochondrial membrane potential

The higher ROS production induces mitochondrial damage. The MMP was determined by using JC-1 fluorescent dye. In apoptotic cells JC-1 forms monomeric units which produce green fluorescence whereas in nonapoptotic cells JC-1 forms aggregate units with red fluorescence. The results showed that Fe_2O_3 NP treatment increased depolarization MMP to 8.52% at 25 µg/ml and 10.74% at 50 µg/ml as compared to 6.35% in untreated cells after 24 h [Figure 9a and b].

Tumorsphere formation

The tumorsphere formation and development ability of MCF-7 cells were investigated in the presence of various concentrations of Fe_2O_3 NPs. The results of the study showed that tumorsphere formation capacity in MCF-7 cells were inhibited by Fe_2O_3 NPs treatment [Figure 10a and b]. The inhibition of MCF-7 tumorsphere formation was 20.50% at 25 µg/ml, 45.12% at 50 µg/ml, and 65.35% at 75 µg/ml concentration, respectively. Thus, treatment with Fe_2O_3 NPs showed a significant inhibition of MCF-7 cell tumorsphere formation at higher concentration.

Discussion

The biosynthesis of NPs using microorganisms such as fungi, bacteria, algae, and actinomycetes is more advantages than

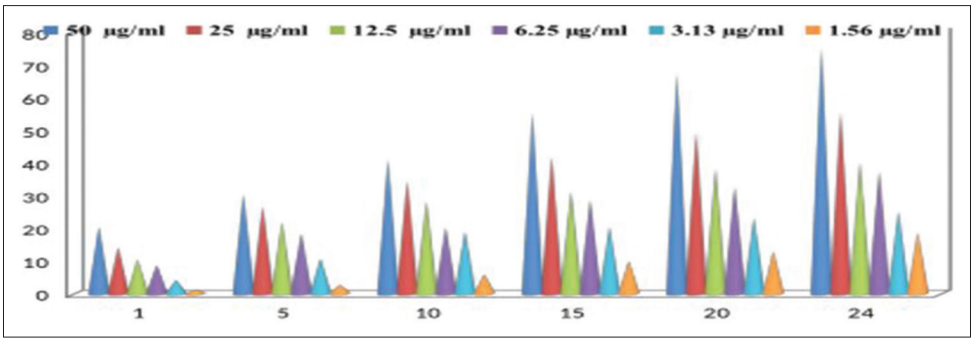

Figure 6: Cytotoxicity effect of Fe2O3 nanoparticle on MCF-7 cancer cells after 24 h of treatment

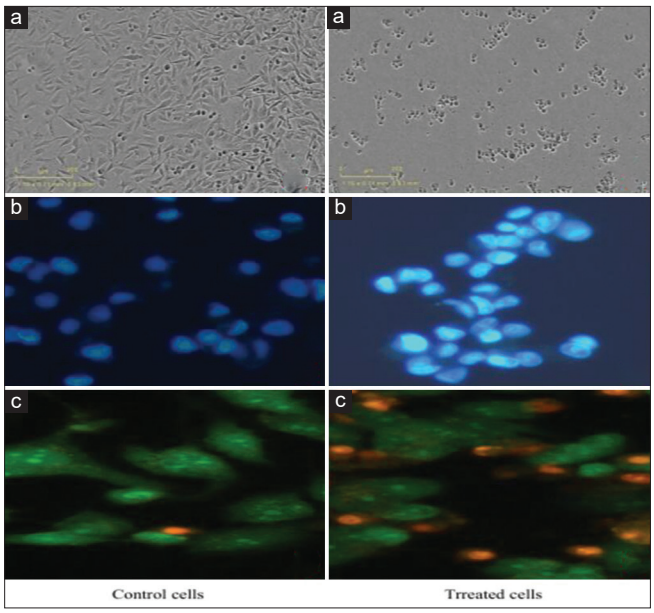

Figure 7: Morphological changes of MCF-7 cells treated with Fe2O3 NP for 24 h viewed under an inverted light microscope (200 x magnification). a) A-Control and treated; b) B Control and treated with DAPI (4, 6-diamidino-2-phenylindole) staining. c) C-Control and treated with acridine orange/ Ethidium bromide stain

physical and chemical methods. Furthermore, biosynthesis method is simple, environmentally safe, and cost-effective with high yield.[16] Fungi contain different types of metabolites, enzymes, proteins, and polysaccharides as reducing agents. The fungus provides large surface area during which enzymes such as nitrate reductase and alpha nicotinamide adenine dinucleotide phosphate oxidase-dependent reductases convert metal salts into metal NPs.[17] The fungal cell wall helps in absorption and reduction of metal NPs. The biosynthesis used fungal biomass and their secondary metabolits is known as myconanotechnology.[18] The fungi used for the production of NP are *Aspergillus terreus, Aspergillus fumigatus, Aspergillus oryzae, Aspergillus niger, Aspergillus flavus, Aspergillus clavatus, Penicillium citrinum, Penicillium janthinellum, Penicillium verrucosum, Penicillium fellutanum, Penicillium chrysogenum, Cladosporium cladosporioides, Agaricus bisporus, Candida albicans, Fusarium oxysporum, Fusarium solani, Fusarium semitectum, Neurospora intermedia, Phomosis sp., Schizosaccharomyces pombe, Shigella dysenteriae, Trichderma versicolor, Trichderma harzianum, Trichderma viride, Trichderma reesei* etc.[19]

In recent years, breast cancer has become a big problem across the whole.[20] Most of the anticancer molecules poses limited approach to kill cancer cells and have side effects.[21] In recent years, NPs have received much attention because of their anticancer activity. Various studies have shown that metal oxide nanoparticles induce cytotoxicity in cancer cells.[22] The green synthesis or biosynthesis of iron oxide NPs using natural material for reducing and capping agents, which are easily available and nontoxic compared to physical and chemical methods are considered as more effective in nanobiotechnology.[23] The surface modification potential and superparamagnetic properties of iron oxide NPs makes them candidate drugs in cancer therapy.[24] The MCF-7 cancer cell line is rapidly proliferating and works as a model to evaluate therapeutic compounds.[24] The Fe_2O_3 NP treatment produces morphological changes during cell death. These morphological modification predicts in breast cancer cells.[25] The Fe_2O_3 NP treatment alters cell morphology which was detected using DAPI and AO/EtBr staining method. The results of MTT assay demonstrated decrease in breast cancer cell viability which was significant at ($P < 0.05$) at higher concentrations. The Fe_2O_3 NP treatment showed antiproliferative potential in breast cancer cells. The Fe_2O_3 NPs treatment on MCF-7 cells inhibits and induces morphological in breast cancer cells. In previous studies, water extract of seaweed (*Sargassum muticum*) were used for the production of iron oxide NPs which exhibit strong cytotoxic effect with IC_{50}-18.75 against MCF-7 cells. Other researchers have shown that cytotoxic effect of Fe_2O_3 NP involves the changes in cellular morphology and disruption of mitochondrial function.[26] The cytotoxicity results of the present study were in accordance with the results of Hilger *et al*.[27] They showed that iron Fe_2O_3 NPs at high concentration reduces the viability of adenocarcinoma cells whereas at low concentration did not produce cytotoxicity. The biologically synthesized Fe_2O_3 NP from ethyl acetate extract display significant cytotoxicity at all the different concentrations.

The ROS generation was estimated using cell permeable DCFH-DA method. The DCFH-DA is an oxidation sensitive fluorescent dye which gets deacetylated by intracellular

esterases into a nonfluorescent DCFH. This nonfluorescent compound is rapidly oxidized by intracellular ROS into a fluorescent 2,7-dichlorofluorescein which is detected by spectrofluorometer. The amount of fluorescence produced is directly proportional to total amount of intracellular ROS level present in cell. The ROS production is an early indicator of apoptosis. The ROS generation in breast cancer cells was examined for 15 h of Fe_2O_3 NP treatment. The loss of MMP predicts mitochondrial dependent cell death. The green fluorescence increases indicating depolarization of mitochondria membrane potential. The disruption of MMP results in red to green fluorescence. Previous findings have shown that the apoptosis is followed by loss of MMP, which results in collapse of electrochemical gradient across the mitochondrial membrane.[28] Our results demonstrated that the Fe_2O_3 NP increased mitochondrial-induced cell death due to ROS production. Previous studies have shown that Fe_2O_3 NP exhibit cytotoxicity changes in cell morphology, mitochondrial disruption, and apoptosis.[26,29,30] Various other reports have shown significant cytotoxicity effect of Fe_2O_3 NP on cancer cells.[26,29,30] The tumorsphere assay is a widely accepted low cost method used for screening the anticancer potential of molecules. The tumorsphere formation was used to further analyze the inhibitory activity of Fe_2O_3 NPs. The biologically synthesized Fe_2O_3 NPs suppressed the tumorsphere formation at all concentrations. The Fe_2O_3 NPs treatment on MCF-7 cells decreased the number and size of the tumorsphere. Further, Fe_2O_3 NP treatment either prevented the MCF-7 tumorsphere formation or decreased the cell viability compared to control. The results obtained showed that Fe_2O_3 NP treatment in breast cancer cells induced ROS production, loss of MMP, and inhibition of tumorsphere formation.

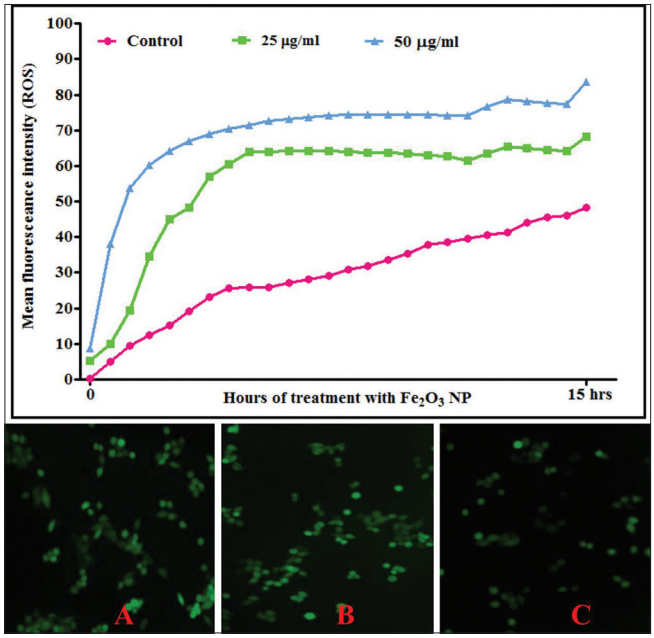

Figure 8a: Measurement of reactive oxygen species (ROS) production in MCF-7 cells treated with Fe2O3 nanoparticles after 15 h. **Figure 8b:** Morphology of MCF-7 cells treated with Fe2O3 nanoparticles for 15 h during reactive oxygen species production. (A-Control, B-25 μg/ml, C - 50 μg/ml concentrations)

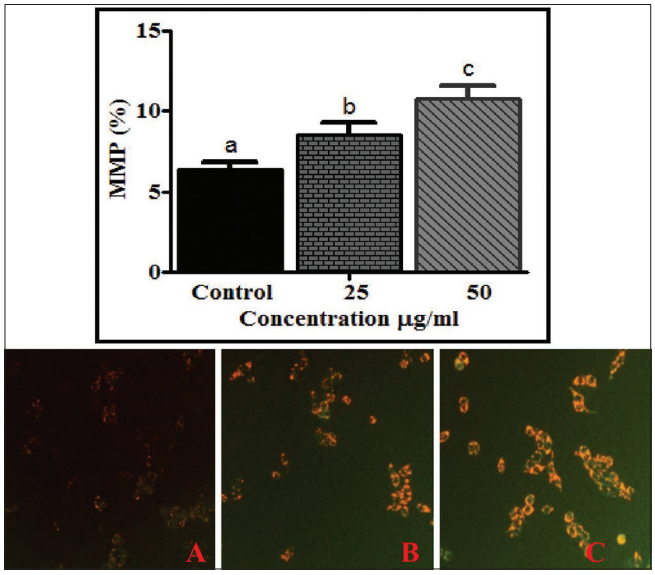

Figure 9a: Depolarization of mitochondrial membrane potential of MCF-7 cells after treatment with Fe2O3 nanoparticles for 24 h
Figure 9b: Morphology of MCF-7 cells treated with Fe2O3 nanoparticles for 24 h during depolarization of mitochondrial membrane potential (A-Control, B-25 μg/ml and C - 50 μg/ml concentrations)

Conclusion

The present study involves the green synthesis of iron oxide NP from *C. cupreum* extract and their *in vitro* anticancer activity. The ethyl acetate extract of *C. cupreum* used for the biosynthesis of Fe_2O_3 NP has various biological activities. The biosynthesis of Fe_2O_3 NP from ethyl acetate extract of *C. cupreum* is economical, simple, and eco-friendly method based on green chemistry approach. In this study, biosynthesis of Fe_2O_3 NP, and its anticancer potential was investigated. The biosynthesized Fe_2O_3 NP showed significant anticancer activity. The results show that the Fe_2O_3 NP increased MMP and ROS production which leads to cell death. Thus, the present study showed significant inhibitory effect on tumorsphere formation. Thus, the biosynthesized Fe_2O_3NP can be used in nanomedicine for the development of therapeutic drug against breast cancer cells.

Acknowledgment

The authors are grateful to the Head, Department of Microbiology and Biotechnology, Bengaluru University, Karnataka, India, for the use of laboratory facilities.

Financial support and sponsorship

The authors are grateful to University Grants Commission, New Delhi, Govt of India for UGC-MRP grants (No-43-474/2014-SR) for financial support.

Conflicts of interest

There are no conflicts of interest.

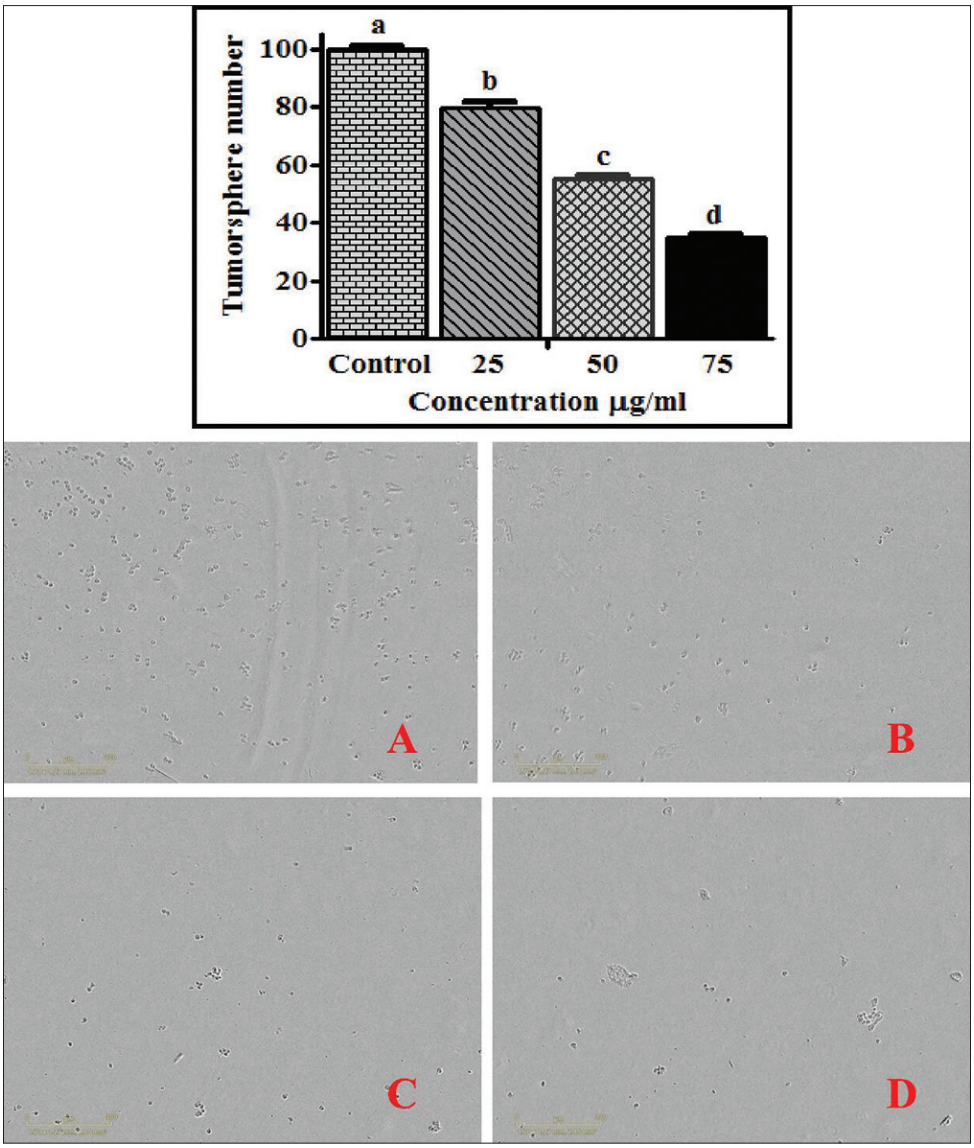

Figure 10a: Fe_2O_3 nanoparticles inhibits tumorsphere formation in MCF-7 cells in a dose dependent manner**. Figure 10b:** Images of Fe_2O_3 nanoparticles inhibits tumorsphere formation in MCF-7 cells. (A-Control, B - 25 μg/ml, C - 50 μg/ml and 75 - μg/ml concentrations)

References

1. Sridhara V, Ali B, Shsziya K, Satapathy LN, Khandelwal P. Biosynthesis and antibacterial activity of silver nanoparticles. Res J Biotechnol 2012;8:11-7.
2. Shankar SS, Rai A, Ahmad A, Sastry M. Rapid synthesis of Au, Ag, and bimetallic Au core-Ag shell nanoparticles using Neem (*Azadirachta indica*) leaf broth. J Colloid Interface Sci 2004;275:496-502.
3. Xie J, Lee JY, Wang DI, Ting YP. Identification of active biomolecules in the high-yield synthesis of single-crystalline gold nanoplates in algal solutions. Small 2007;3:672-82.
4. Wang T, Jin X, Chen Z, Megharaj M, Naidu R. Green synthesis of Fe nanoparticles using eucalyptus leaf extracts for treatment of eutrophic wastewater. Sci Total Environ 2014;466-467:210-3.
5. Kumar R, Roopan SM, Prabhakarn A, Khanna VG, Chakroborty S. Agricultural waste *Annona squamosa* peel extract: Biosynthesis of silver nanoparticles. Spectrochim Acta A Mol Biomol Spectrosc 2012;90:173-6.
6. Roopan SM, Bharathi A, Prabhakarn A, Rahuman AA, Velayutham K, Rajakumar G, *et al*. Efficient phyto-synthesis and structural characterization of rutile TiO2 nanoparticles using *Annona squamosa* peel extract. Spectrochim Acta A Mol Biomol Spectrosc 2012;98:86-90.
7. Sastry M, Ahmad A, Islam KM, Kumar R. Biosynthesis of metal nanoparticles using fungi and actinomycete. Curr Sci 2003;85:162-70.
8. Wang ZW, Gu MY, Li GZ. Surface properties of gleditsia saponin and synergisms of its binary system. J Disper Sci Technol 2005;26:341-7.
9. Pande JS. Text Book of Botony Diversity of Microbes and Cryptogams. Gangotri, India: Rastogi Publications; 2008. p. 308-10.
10. Nazir AW, Sharmila T. Evaluation of antioxidant properties of different extracts of *Chaetomium cupreum* SS02. Bull Fac Pharm Cairo Univ 2018;56:191-8.
11. Shahwan T, Abusirriah S, Nairat M, Boyac E, Eroglu AE, Scott TB, *et al*. Green synthesis of iron nanoparticles and their application as a Fenton-like catalyst for the degradation of aqueous cationic and anionic dyes. Chem Eng J 2011;172:258-66.
12. Mosmann T. Rapid colorimetric assay for cellular growth and survival: Application to proliferation and cytotoxicity assays. J Immunol Methods 1983;65:55-63.
13. LeBel CP, Ischiropoulos H, Bondy SC. Evaluation of the probe 2',7'-dichlorofluorescin as an indicator of reactive oxygen species formation and oxidative stress. Chem Res Toxicol 1992;5:227-31.
14. Saleem MZ, Nisar MA, Alshwmi M, Din SR, Gamallat Y, Khan M,

et al. Brevilin A inhibits STAT3 signaling and induces ROS-dependent apoptosis, mitochondrial stress and endoplasmic reticulum stress in MCF-7 breast cancer cells. Onco Targets Ther 2020;13:435-50.
15. Lu Y, Ma W, Mao J, Yu X, Hou Z, Fan S, *et al*. Salinomycin exerts anticancer effects on human breast carcinoma MCF-7 cancer stem cells via modulation of Hedgehog signaling. Chem Biol Interact 2015;228:100-7.
16. Kumar V, Yadav SK. Plant-mediated synthesis of silver and gold nanoparticles and their applications. J Chem Technol Biotechnol 2009;84:151-7.
17. Shah M, Fawcett D, Sharma S, Tripathy SK, Poinern GE. Green synthesis of metallic nanoparticles via biological entities. Materials (Basel) 2015;8:7278-308.
18. Gade A, Ingle A, Whiteley C, Rai M. Mycogenic metal nanoparticles: Progress and applications. Biotechnol Lett 2010;32:593-600.
19. Khan AU, Malik N, Khan M, Cho MH, Khan MM. Fungi-assisted silver nanoparticle synthesis and their applications. Bioprocess Biosyst Eng 2018;41:1-20.
20. Karia P, Patel KV, Rathod SS. Breast cancer amelioration by *Butea monosperma* in-vitro and in-vivo. J Ethnopharmacol 2018;217:54-62.
21. Ji HF, Li XJ, Zhang HY. Natural products and drug discovery. Can thousands of years of ancient medical knowledge lead us to new and powerful drug combinations in the fight against cancer and dementia? EMBO Rep 2009;10:194-200.
22. Jayapaul J, Hodenius M, Arns S. FMN-coated fluorescent iron oxide nanoparticles for RCP-mediated targeting and labeling of metabolically active cancer and endothelial cells. Biomaterials 2011;32:5863-71.
23. Santhosh PB, Ulrih NP. Multifunctional superparamagnetic iron oxide nanoparticles: Promising tools in cancer theranostics. Cancer Lett 2013;336:8-17.
24. Lin KL, Tsai PC, Hsieh CY, Chang LS, Lin SR. Antimetastatic effect and mechanism of ovatodiolide in MDA-MB-231 human breast cancer cells. Chem Biol Interact 2011;194:148-58.
25. Stewart BW. Mechanisms of apoptosis: Integration of genetic, biochemical, and cellular indicators. J Natl Cancer Inst 1994;86:1286-96.
26. Willner I, Willner B. Functional nanoparticle architectures for sensoric, optoelectronic, and bioelectronic applications. Pure Appl Chem 2002;74:1773-83.
27. Hilger I, Fruhauf S, Lin W. Cytotoxicity of selected magnetic fluids on human adenocarcinoma cells. J Magn Magn Mater 2003;261:7-12.
28. Bras M, Queenan B, Susin SA. Programmed cell death via mitochondria: Different modes of dying. Biochemistry (Mosc) 2005;70:231-9.
29. Moghimi SM, Hunter AC, Murray JC. Long-circulating and target-specific nanoparticles: Theory to practice. Pharmacol Rev 2001;53:283-318.
30. Dresco PA, Zaitsev VS, Gambino RJ, Chu B. Preparation and properties of magnetite and polymer magnetite nanoparticles. Langmuir 1999;15:1945-51.